Analytical Biochemistry 402 (2010) 170–178

Contents lists available at ScienceDirect

Analytical Biochemistry

journal homepage: www.elsevier.com/locate/yabio

Kinetic analysis and fragment screening with Fujifilm AP-3000

Rebecca L. Rich, David G. Myszka *

Center for Biomolecular Interaction Analysis, University of Utah School of Medicine, Salt Lake City, UT 84132, USA

ARTICLE INFO

Article history:
Received 7 January 2010
Received in revised form 30 March 2010
Accepted 31 March 2010
Available online 3 April 2010

Keywords:
Protein–protein
Kinetics
Surface plasmon resonance

ABSTRACT

We evaluated the performance of Fujifilm's new AP-3000 surface plasmon resonance biosensor for kinetic analysis and fragment screening. Using carbonic anhydrase II as a model system, we characterized a set of 10 sulfonamide-based inhibitors that range in molecular mass from 98 to 341 Da and approximately 10,000-fold in affinity (0.4 mM to 20 nM). Although the data collected from the AP-3000 were generally similar to those collected using a Biacore T100, the AP-3000's stop-flow analyte delivery system complicated the shapes of the association- and dissociation-phase binding responses. We illustrate how reasonable estimates of the kinetic rate constants can be extracted from AP-3000 data by limiting data analysis to only the regions of the responses collected during flow conditions. We also provide an example of the results obtained for a fragment-screening study with the AP-3000, which is the ideal application of this technology.

Having worked in the field of biosensor technology for nearly 20 years, we are often asked to evaluate emerging biosensor systems [1–6]. In this regard, we recently had the opportunity to work with the AP-3000, a new surface plasmon resonance-based biosensor developed by Fujifilm [7,8]. Noting that the company promotes the instrument as a "drug-screening system," we focused our evaluation on the instrument's ability to directly detect small-molecule binding interactions.

We used carbonic anhydrase II (CAII),[1] one of our favorite targets to work with as a model system. We developed this system roughly 10 years ago as part of a DARPA (Defense Advanced Research Projects Agency) program to help evaluate sensor technology. The system has come in handy to help validate surface-based binding constants [9] and thermodynamics [10] as well as to demonstrate how to interpret mass transport-limited reactions measured using biosensors [11]. In fact, we have seen CAII adopted by a number of users to help evaluate other sensor technologies and as a training tool. The protein is commercially available, easy to work with, and highly active in terms of binding activity. In addition, a variety of its small-molecule inhibitors, ranging both in size and in several orders of magnitude in affinity and association/dissociation kinetics, are readily soluble, stable over time, and commercially available.

The heart of the AP-3000 is its use of sensor sticks, which are configured with 12 separate flow cells. The flow cells are grouped in pairs, with 6 serving as reaction surfaces and 6 serving as reference surfaces. Six analyte samples are assayed in parallel using a pipette delivery system, employing what Fujifilm describes as a stop-flow method. Samples are actually pipetted into the flow cell under flow for a short period of time (~10 s) and then the flow is stopped, leaving binding interactions to occur under diffusion control only. Similarly, during the dissociation phase, the flow cell is initially washed under flow with buffer for approximately 10 s and then the flow is again stopped.

We wanted to assess specifically how this stop-flow delivery method would affect binding responses. We chose to directly compare the binding results obtained from the AP-3000 with those obtained by a Biacore T100. In contrast to the AP-3000, the T100 uses a constant flow system, meaning that the analyte is delivered by flow during the association phase and the surface is constantly washed with buffer under flow during the entire dissociation phase.

To take advantage of the streptavidin (SA)-based sensor sticks available with the AP-3000, we chose to minimally biotinylate the CAII for these studies. The same protein and analyte samples were tested using both the AP-3000 and T100 under identical conditions. As one might expect, we found that the use of the stop-flow method in the AP-3000 complicates the shapes of the association and dissociation responses, particularly as the association rate constant increases. But by limiting the kinetic analysis to the portions of data collected under flow, we found a good correlation for the kinetics determined from the AP-3000 and T100.

Because the AP-3000 is promoted as a drug-screening system, we also ran a fragment-screening assay against CAII using a 3500-compound library. We illustrate the processing steps

* Corresponding author. Fax: +1 801 585 3015.
E-mail address: dmyszka@cores.utah.edu (D.G. Myszka).

[1] *Abbreviations used:* CAII, carbonic anhydrase II; SA, streptavidin; PBS, phosphate-buffered saline; DMSO, dimethyl sulfoxide; NHS, *N*-hydroxysuccinimide; LC, liquid chromatography; bCAII, biotinylated CAII; RU, resonance units.

0003-2697/$ - see front matter © 2010 Elsevier Inc. All rights reserved.
doi:10.1016/j.ab.2010.03.043

required to account for drifting baselines and loss of target activity, which are common in long experimental runs. We found that the high-capacity SA-based sensor sticks, in combination with the instrument's ability to test 10 384-well plates in 24 h, make the AP-3000 worthy of its claim to be a drug-screening system.

Materials and methods

Binding studies were performed at 19 °C using Fujifilm AP-3000 and Biacore T100 optical biosensors equilibrated with running buffer (Dulbecco's Ca^{2+}- and Mg^{2+}-free phosphate-buffered saline [PBS] supplemented with 1% dimethyl sulfoxide [DMSO]). The AP-3000 biosensor, SA-401 sensor sticks, and other instrument-specific consumables (including 384-well plates, protein plates, and pipette tips) were obtained from Fujifilm Japan. CM5 sensor chips and Biacore consumables were obtained from GE Healthcare. SA and EZ-Link sulfo-NHS-LC-LC-biotin were purchased from Pierce. CAII, sulfonamides, and general laboratory reagents were obtained from Sigma. Fragment libraries were obtained from Maybridge and Active Site.

Target biotinylation

CAII was dissolved in PBS at 1 mg/ml (~30 μM). Sulfo-NHS-LC-LC-biotin was added at a 0.5 M ratio to ensure minimal biotinylation. After incubation for 3 h at 4 °C, free biotin was removed by passing the solution through a Superdex 75 gel filtration column.

Target captures

Biotinylated CAII (bCAII) was diluted to 0.01 mg/ml and captured on a Fujifilm SA-401 sensor stick with sample swing for 1 h. The same bCAII solution was also captured on a Biacore T100 CM5 sensor chip prederivatized with 12,000 resonance units (RU) of SA.

Kinetic analyses

CAII small-molecule inhibitors were tested in 3-fold dilution series using a 55-s contact time in both AP-3000 and T100 experiments. For the T100, samples were injected at 40 μl/min and responses were monitored for a 3-min dissociation phase. Four washing cycles were used in the AP-3000 dissociation phase. Each compound was assayed in a seven-sample concentration series using 3-fold dilutions starting at 1.67 mM (methanesulfonamide), 1 mM (sulpiride), 330 μM (sulfanilamide), 5 μM (acetazolamide), and 50 μM (the other sulfonamides). Each concentration series was run in duplicate using the T100 and in quadruplicate using the AP-3000. Data were collected from both instruments at 19 °C. An internal two-point DMSO calibration curve (running buffer with 1.25% and 0.75% DMSO) was used to correct for excluded volume effects.

Data processing and analysis of kinetic data

Response data from both the T100 and AP-3000 were processed using Scrubber (BioLogic Software). Responses were zeroed before the start of the analyte injections, then reference subtracted, and finally double referenced using blank injections. The AP-3000 data were also despiked using the despike option in Scrubber. To extract binding constants, the data sets from each instrument were globally fit to a 1:1 interaction model that included a mass transport term. The entire association and dissociation phases were fit for the T100 data. For the AP-3000 data, only the initial 10 s of the association and dissociation phases was fit.

Fragment screening

Using the AP-3000, a total of 3800 compounds from the Maybridge and Active Site libraries were screened at a concentration of 100 μM against bCAII. Sulpiride was tested as a positive control at 1 mM after every 64 cycles in each flow cell. A calibration series of eight samples ranging from 0.95% to 1.15% DMSO in running buffer was tested at the beginning and end of the screen. Because screening of 10×384 sample plates required two separate AP-3000 sensor sticks, bCAII was captured on each stick using 1 h of swinging contact time.

Data processing and analysis of screening data

Fragment screening data were processed by subtracting reference surface responses. Report points at an average of 40 to 50 s into the association phase were further processed by first normalizing the baseline. Baseline normalization was done by subtracting the mean response using a window of 10 data points. The loss of control binding activity was normalized by fitting a two-parameter polynomial to the response for the control and dividing this response across the entire sample set.

Results

Capture of biotinylated target

The first step in configuring a biosensor assay is to attach the target protein onto the sensor surface. Because the AP-3000's SA sensor sticks are designed to work with biotinylated targets, we minimally biotinylated the CAII using sulfo-NHS-LC-LC-biotin. Fig. 1 shows the capturing step for the bCAII run in parallel in all six channels of the AP-3000 sensor stick. Each flow cell required approximately 70 μl of target for capture.

During the capturing phase, the target solution is repeatedly pushed and pulled over the sensor surfaces in what Fujifilm describes as "swinging." This method of flowing the ligand provides more efficient transfer of ligand to the surface than a static system and minimizes sample consumption by effectively recirculating the sample. The capturing time can be controlled to be as short as 1 min to as long as 1 h. For these experiments, the target was swung for 1 h to maximize its capture level. After target capture, the surfaces were blocked with soluble biotin and washed with buffer, producing the sawtoothed jumps in response observed at a time of approximately 4000 to 4500 s in Fig. 1.

Fig. 1 also illustrates that bCAII was captured to similar levels (~16,000 RU) in each of the six flow cells. In fact, the capture densities varied by less than 3%. Because we would be comparing analyte binding between the six target surfaces, it was critical that the surfaces had the same density of target captured.

For the T100 studies, the same bCAII sample was captured on a CM5 sensor chip derivatized with approximately 12,000 RU of SA. The total target capture level for the T100 experiment was 6000 RU, which was roughly three times less than that with the AP-3000.

Processing of AP-3000 data

Because the AP-3000 data processing and analysis software was not capable of double referencing, auto-alignment, or kinetic analysis, we worked with BioLogic Software to develop a version of their Scrubber analysis software package to handle AP-3000-specific data. Unlike the standard version of Scrubber, this new version, called ScrubberFF, needed to import and process data collected simultaneously from six reaction surfaces and six reference surfaces.

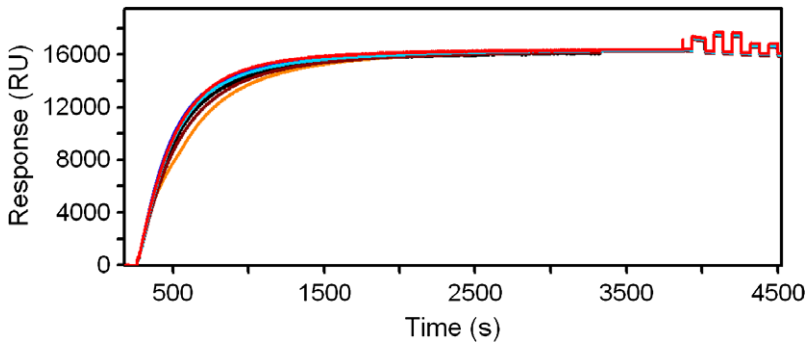

Fig. 1. Capture of biotinylated target on the six reaction flow cells of an AP-3000 SA-coated sensor stick.

Because the data processing methodology for the AP-3000 is new, here we illustrate the main steps of the process using data collected for the CAII inhibitor sulpiride. Sulpiride (341 Da) was tested in a 3-fold dilution series for a total of seven concentrations using 1 mM as the highest concentration. The entire concentration series was tested eight times.

Fig. 2A shows an overlay of the raw data collected from reaction flow cell 1 and reference flow cell 1. The group of data that starts around 73,000 RU in response represents the data sets from the reference surface. The data grouped around 85,000 RU in response are from the reaction surface. The baseline responses from the reaction surface are higher because this surface is coated with bCAII. Also, the start of the analyte injections (indicated by the jump in signal) occurs approximately 12 s later on the reaction surface compared with the reference surface. This is because an analyte is first injected over the reference surface and then is injected over the reaction surface. Similarly, during the dissociation phase, buffer is first washed over the reference surface and then over the reaction surface. This delay between injections across the reference and reaction flow cells can be corrected for during data processing.

The first step in data processing is to zero the response data just prior to the analyte injections. This was done for the data shown in Fig. 2A by selecting a 10-s window just prior to the start of the analyte injections and setting the responses in this window to $y = 0$. Next, the responses from the reference and reaction were aligned on the x axis (Fig. 2B) to account for the delay between the two as mentioned above. Scrubber automatically identifies the steepest slope caused by the mismatch between the running buffer and analyte to align the start of the injection to zero on the x axis. Fortunately, aligning the injection start does a reasonably good job of also aligning the start of the dissociation phase, so no further adjustments in the alignment were needed.

Once the data have been normalized, we begin to see the concentration-dependent responses for sulpiride (Fig. 2B). And even at this stage of the process, we can see that the bound sulpiride rapidly dissociates from the protein surface, returning the signal to baseline during the washout phase.

The next step in data processing is to subtract the response that is collected on the reference surface from the corresponding reaction surface. This was done automatically in ScrubberFF for each injection, resulting in the corrected responses shown in Fig. 2C. We see how referencing has further improved the quality of the data by removing bulk refractive index changes and some drift. Fig. 2C also demonstrates the reproducibility of the system. In this panel, the eight replicate tests of the sulpiride concentration series (each shown as a different color) overlay extremely well.

In Fig. 2C, however, we do notice a downward jump in the response at approximately 10 s into the start of both the association and dissociation phases. This jump is caused by the injection tips moving into and out of the ports of the reference and reaction flow cells. Because the timing and magnitude of the jumps are fairly consistent and these jumps occur even with plain buffer injections, we can use the information from buffer injections to remove this artifact in a processing step we call double referencing [12]. Therefore, we averaged the responses from the blank injections and subtracted this average from the entire data set, resulting in the double-referenced responses shown in Fig. 2D. Note that the jumps in the responses are now gone.

The final data processing step is to remove unwanted spikes, which often occur at the beginning and end of the analyte injection step, from the responses. These spikes, which typically constitute a single data point, were removed using the automatic despike function in ScrubberFF. Scrubber identifies the spikes by looking for outlier points in each data set.

Fig. 2E shows the final processed data set for sulpiride from a single flow cell in the AP-3000. The overlay of the eight replicate data sets indicates that the bCAII surface did not lose activity during the assay. The sulpiride binding response also returned back to baseline during a single washing step, indicating that this compound dissociated completely from the target surface within the first few seconds of the dissociation phase. This rapid return to baseline occurred because sulpiride has a relatively fast dissociation rate constant and a relatively slow association rate constant. Not all of the CAII inhibitors we studied behaved this well, as we discuss below.

Comparative analysis of data from the AP-3000 and T100

Fig. 3 shows the response data for 10 CAII inhibitors from the T100 and AP-3000 plotted side by side. Each compound was tested in a 3-fold dilution series. With the T100, the entire assay was run in duplicate; using the AP-3000's faster sampling speed, we tested each analyte concentration in quadruplicate in approximately 24 h. The T100 analyses included a 3-min dissociation phase, and the AP-3000 used four dissociation-phase wash cycles.

When one visually compares all of the data from the two instruments, two general observations can be made. First, the replicate responses overlay, demonstrating the reproducibility of data obtained from both instruments. Second, the shapes of the responses are comparable between the two assays for individual compounds.

In fact, even the data for the smallest and lowest affinity compound we studied (methanesulfonamide, compound 1, 98 Da) gave similar-shaped binding responses from the T100 and AP-3000. The compound that deviates the most between the two instruments is acetazolamide (compound 10 in Fig. 3). As we have shown previously, acetazolamide actually displays a very fast association rate and high affinity for CAII [13]. This complicates the AP-3000 data because the compound does not dissociate from the surface completely before the next concentration in the analyte series is tested. We have more to say about the results for this compound later.

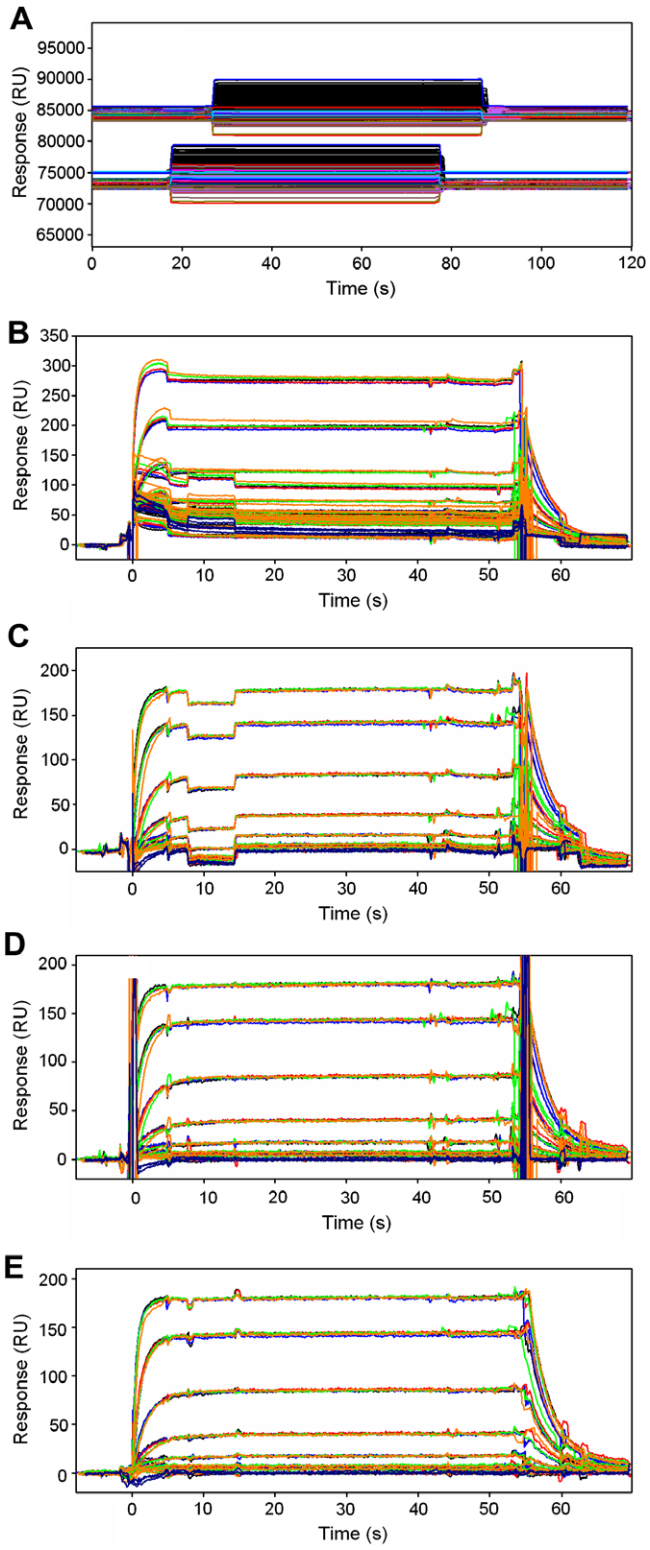

Fig. 2. Data processing steps for the AP-3000. (A) Zeroing on the *y* axis. (B) Aligning to $t = 0$. (C) Subtracting responses from reference surface. (D) Subtracting responses from blank buffer injections. (E) Despiking the data set. For simplicity, shown here are only the responses from a single reaction flow cell. The eight replicate analyses of a sulpiride concentration series (1 mM was the highest concentration in a 3-fold dilution series of seven total concentrations) are shown as different colors. (For interpretation of the reference to color in this figure legend, the reader is referred to the Web version of this article.)

But if one looks very carefully at the AP-3000 dissociation-phase data in particular, one will notice that most of the compounds show a complex "stepped-down" profile (as opposed to the smooth exponential decay that is observed in the T100 data). In fact, the kinetics of both the AP-3000 association and dissociation phase data is complicated by the stop-flow injection procedure.

Kinetic analysis of AP-3000 data

Our standard approach with kinetic analysis is to globally fit all of the response data collected during the association and dissociation phases [14]. For example, Fig. 4A shows a global fit of the data for 1,3-benzenedisulfonamide collected using the T100. The full binding cycle for each concentration is well described by a 1:1 interaction model.

However, we are not able to use the approach of globally fitting all of the AP-3000 data because the response data are complicated by the stop-flow method. To highlight this effect, we first focus on the dissociation phase for 1,3-benzenedisulfonamide collected from the AP-3000 (Fig. 4B).

Unlike the T100 (which maintains constant fluid flow throughout a binding cycle), the AP-3000 cycles between periods of fluid flow and no flow (flow periods are indicated by the teal bars in Fig. 4B). During the association phase, the analyte is actually introduced with flow for only a short period of time (~10 s) and then the flow is stopped. Multiple periods of flow/no flow occur during the dissociation phase as buffer is introduced over the surfaces to remove analyte. Fully dissociating 1,3-benzenedisulfonamide from the AP-3000 surface required all four sequential washing steps.

It is not surprising that during the periods of flow, we observe a significantly faster association and dissociation rate due to mass transport. Under no-flow conditions, the binding rates become completely diffusion controlled and, therefore, are slowed down during both the association and dissociation phases.

Although it may be possible to globally fit an entire data set collected from the AP-3000 using a model that includes different transport rates in regions of flow and no flow, we decided to take a simpler approach at this time. Instead of fitting all of the data, we globally fit a limited region of the data set, specifically the areas that are under flow conditions ($t = 0$–10 s during the association phase and 55–65 s during the dissociation phase). An example of fitting the 1,3-benzenedisulfonamide data is shown by the red lines in Fig. 4B. The same fitting procedure was applied to the data shown in Fig. 3 for all 10 compounds.

Comparison of T100 and AP-3000 binding kinetics

Fig. 5A and B shows correlation plots of the association and dissociation kinetics, respectively, for all 10 compounds determined from the T100 versus the AP-3000. A table of the binding constants is provided in Supplementary material. The correlation coefficients for the association and dissociation rates were 0.958 and 0.997, respectively. Given the limitations introduced by the stop-flow method in the AP-3000, we were pleased to see the rate constants correlated so well. This was clearly the result of limiting our interpretation to areas of the AP-3000 data that were collected under flow conditions.

The compound with the biggest deviation in the association rate was acetazolamide. This is not surprising given that this compound has the fastest association rate. Also, as mentioned earlier, acetazolamide does not completely dissociate from the surface during the washout steps, further complicating the analysis. We are interested in seeing whether a better correlation can be obtained for this compound using regenerated surfaces, which we are currently investigating.

Fig. 6 shows a correlation plot of the K_D values determined from the kinetic analysis of the AP-3000 and T100 data. Given that the rate constants correlate well, it is not surprising that the affinities

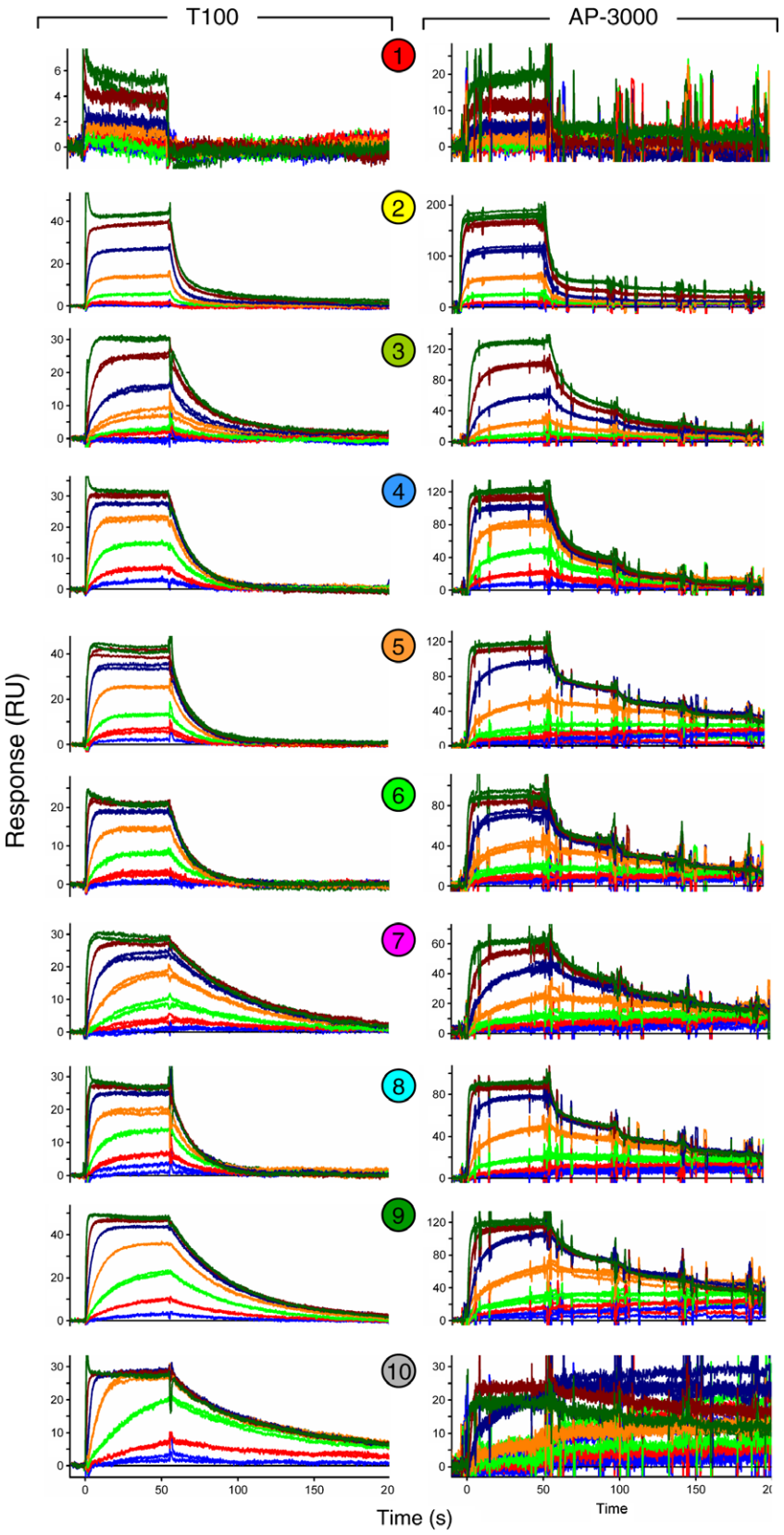

Fig. 3. Responses for concentration series of 10 sulfonamide/CAII interactions measured using Biacore T100 (left) and Fujifilm AP-3000 (right): (1) methanesulfonamide, (2) sulpiride, (3) 4-aminomethylbenzenesulfonamide, (4) sulfanilamide, (5) dansylamide, (6) benzenesulfonamide, (7) 4-carboxybenzenesulfonamide, (8) 1,3-benzenedisulfonamide, (9) furosemide, and (10) acetazolamide. Each compound was assayed in a seven-sample concentration series using 3-fold dilutions starting at 1.67 mM (methanesulfonamide), 1.0 mM (sulpiride), 330 μM (sulfanilamide), 5 μM (acetazolamide), and 50 μM (the other sulfonamides). Each concentration series was run in duplicate using the T100 and in quadruplicate using the AP-3000.

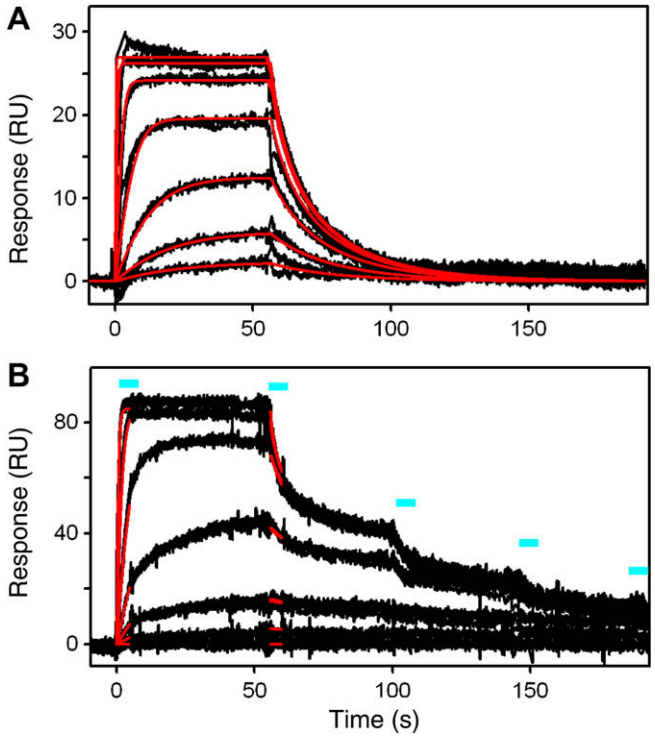

Fig. 4. Responses for the 1,3-benzenedisulfonamide/CAII interaction measured using Biacore T100 (A) and Fujifilm AP-3000 (B). 1,3-Benzenedisulfonamide was tested in replicate in a 3-fold dilution series starting at 50 μM. The red lines depict the fit of a 1:1 interaction model that includes a mass transport term. In panel B, the teal bars indicate time periods when analyte or buffer is flowing across the surface. (For interpretation of the references to color in this figure legend, the reader is referred to the Web version of this article.)

gave a correlation coefficient of 0.994. Again for the reasons discussed above, the biggest outlier was acetazolamide, which has the fastest association rate. But overall, we were pleased with the correlation in affinities for these compounds, which ranged more than 10,000-fold in K_D values.

Fragment screening with the AP-3000

Although we demonstrated that it is possible to extract reliable binding constants from the AP-3000 data, the instrument was designed primarily as a screening platform. To evaluate it in this role, we screened 10 × 384-well plates of samples in 24 h (which is the setup limit of the current instrument). We ran compounds from a combination of the Maybridge and Active Site fragment libraries at a concentration of 100 μM, a concentration we typically use when performing fragment screens. As a control to monitor activity of the target surface, we also tested sulpiride (at 1 mM) after every 64 assay cycles.

Fig. 7 shows the processed response data collected from flow cell 1 throughout the first five plates of the screening assay. The data for the control compound sulpiride is represented by the purple lines. To track surface activity and potential hits to the target, we used ScrubberFF to report an averaged response for each curve between 60 and 70 s (indicated by the red box).

The responses for the report points were plotted versus injection number in a trend plot (Fig. 8A). This trend plot displays an overlay of the response data collected in parallel from each of the six reaction flow cells. The first thing to notice is that the response for the control compound sulpiride is fairly consistent in magnitude across the six flow cells. The signal for sulpiride decreased slowly during the screen, likely reflecting the loss of activity of the captured bCAII target over many assays. The number of assays possible on a single sensor stick under our current assay condition was five 384-well plates. This limitation is set by the AP-3000 and is related to the number of times the pipette tips are able to dock into a sensor stick.

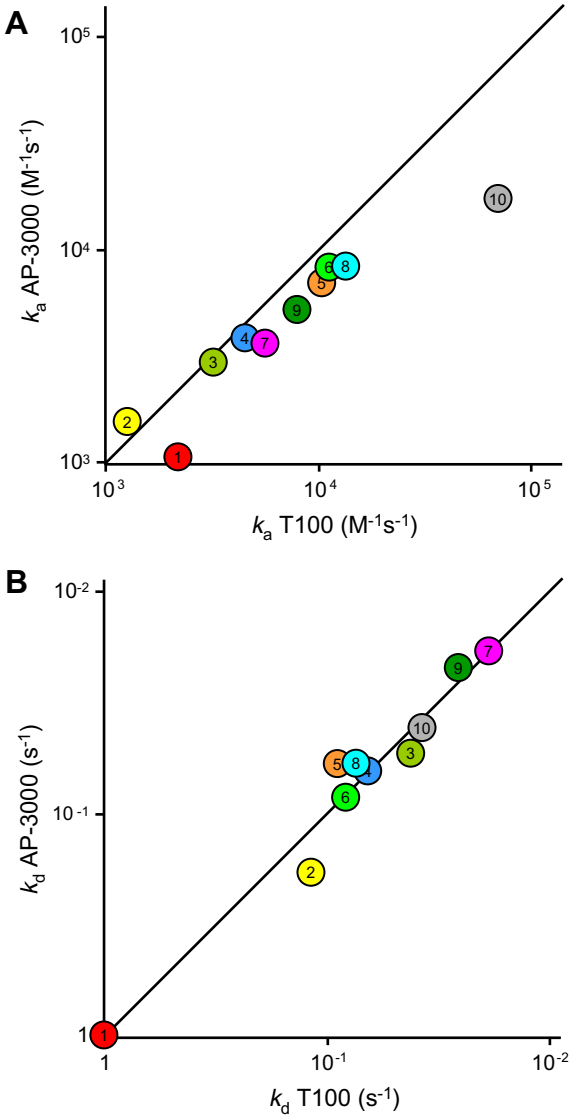

Fig. 5. Correlation plots from AP-3000 and T100 of association rate constants (A) and dissociation rate constants (B) determined using kinetic analysis. In both plots, a correlation of 1 is indicated by the diagonal line.

Once the analysis of the fifth plate was completed, the instrument automatically captured another aliquot of bCAII onto a new SA sensor stick and used this fresh stick to complete the analysis of plates 6 to 10. This causes the signal for sulpiride to appear to jump in response and then decay again at a similar rate, as was observed when assaying the first five sample plates. The fact that the signal increased for sulpiride on the new sensor stick provides evidence that the target protein on the first stick (bCAII), rather than the control compound in solution (sulpiride), was losing activity over time.

The level of signal decay shown in Fig. 8 is reasonable and can be accounted for during data processing, as described below. However, if a target is significantly less stable, it is possible to limit the assay number applied to each sensor stick so as to minimize the amount of data collected on a low-activity surface. (It should be noted that biotinylated ligands are stored in a temperature-controlled plate within the instrument prior to immobilization to help

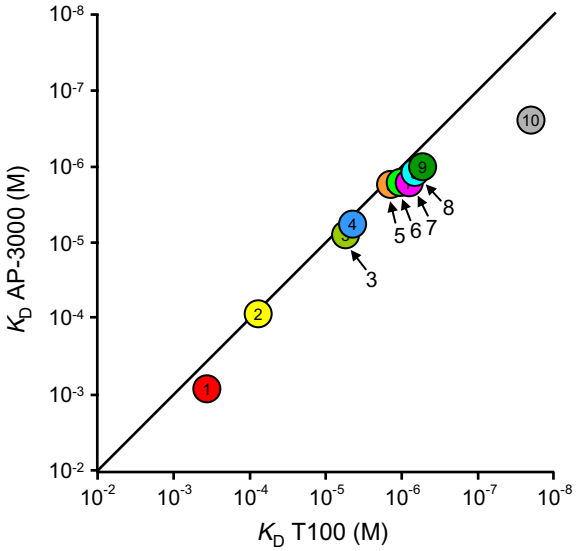

Fig. 6. Correlation plots of the 10 compounds' affinities determined from the kinetic analysis. A correlation of 1 is indicated by the diagonal line.

improve their stability.) The AP-3000 can hold up to four sensor sticks, which can be configured for automated immobilizations within a single run.

The first processing step we applied to the trend plot data was to normalize the baseline from each flow cell and each sensor stick. This was done by subtracting the median of the data using a window of 10 data points. The resulting baseline-corrected data are shown in Fig. 8B. Next, we fit the response data for the control compound sulpiride to a two-parameter polynomial (shown by the black curves). These polynomials were then used to normalize the response data from each corresponding flow cell, producing the normalized data sets shown in Fig. 8C.

The top orange line in Fig. 8C indicates the response of the control compound sulpiride from each flow cell normalized to 100. The data points surrounded by stars represent responses for four known sulfonamide-based compounds, which were purposefully placed within the sample set. The fact that these compounds show up as reproducible hits within the assay (and across sensor sticks) helps to further validate the performance of the screening assay. We identified approximately 100 potential hits that we are currently following up on by testing them in full concentration series against CAII, as well as other control proteins, to see whether they are specific binders.

Discussion

Being fairly devoted users of biosensor technology, we are excited to see the number and variety of commercially available biosensor instruments increasing. In fact, based on our recent survey of the literature, there are currently approximately 30 different manufacturers of label-free systems [15]. And as the biosensor field matures, we are witnessing a trend toward systems that are dedicated for more specific applications. A good example of this is the new AP-3000 from Fujifilm. This system has been engineered with a focus on drug discovery and, in particular, on fragment-screening applications.

Given the potential of the AP-3000, we investigated how well it could perform in terms of sensitivity, reproducibility, and speed. For capture on the SA sensor sticks, we could employ biotinylation of the target protein, which is one of our preferred methods for tethering proteins to a sensor surface. We also found that the SA sticks for the AP-3000 have exceptionally high binding capacity for biotinylated proteins (RU capture levels ranged from 18,000 to 22,000 RU for typical proteins). This, of course, is an essential requirement for small-molecule analysis; the more active binding sites on the surface, the bigger the signal. The ability to use swinging during the capturing phase allowed us to expose a small volume of biotinylated ligand to the sensor surface for as long as 1 h, thereby lowering our target consumption.

We used 10 sulfonamide-based inhibitors of CAII, which have a range of binding association and dissociation kinetics, to probe the reliability of the AP-3000. We found the binding responses to be exceptionally reproducible. We found that the AP-3000 has sensitivity capable of detecting small molecules (<100 Da) as well as weakly bound ones (K_D > 500 μM), a requirement for successful fragment screening. However, we demonstrated that the use of the stop-flow system for sample introduction can complicate the binding responses in both the association and dissociation phases. Because of mass transport, this complexity becomes more pronounced as the association rates of the analytes increase. But by limiting the analysis of the kinetics to the regions of data collected under flow conditions, we showed that it is possible to extract reliable kinetic rate constants from the AP-3000 data.

Because the main application of the AP-3000 is for drug screening (and fragment screening in particular), the issues introduced by the stop-flow method are less critical. In fragment screening, for

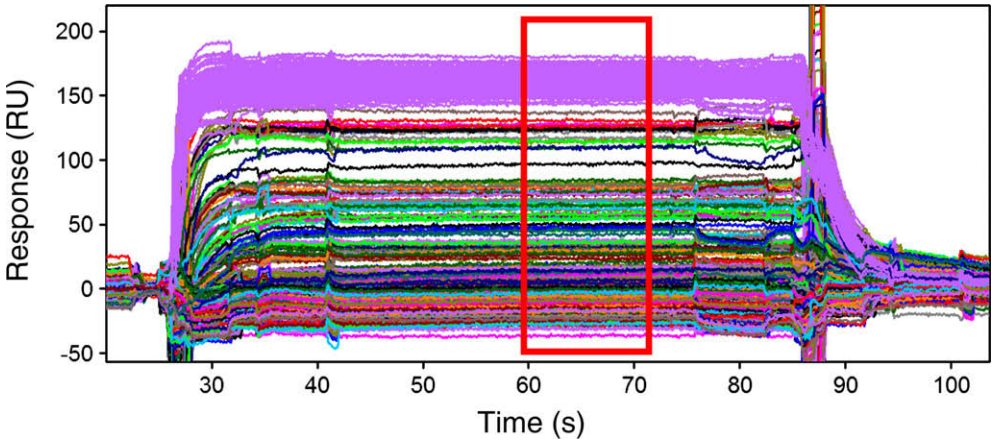

Fig. 7. Overlaid responses from the AP-3000 screen of five 384-well compound plates from flow cell 1. Replicate responses of the positive control are shown in purple. Responses highlighted by the red box were used to produce the plots in Fig. 8. (For interpretation of the references to color in this figure legend, the reader is referred to the Web version of this article.)

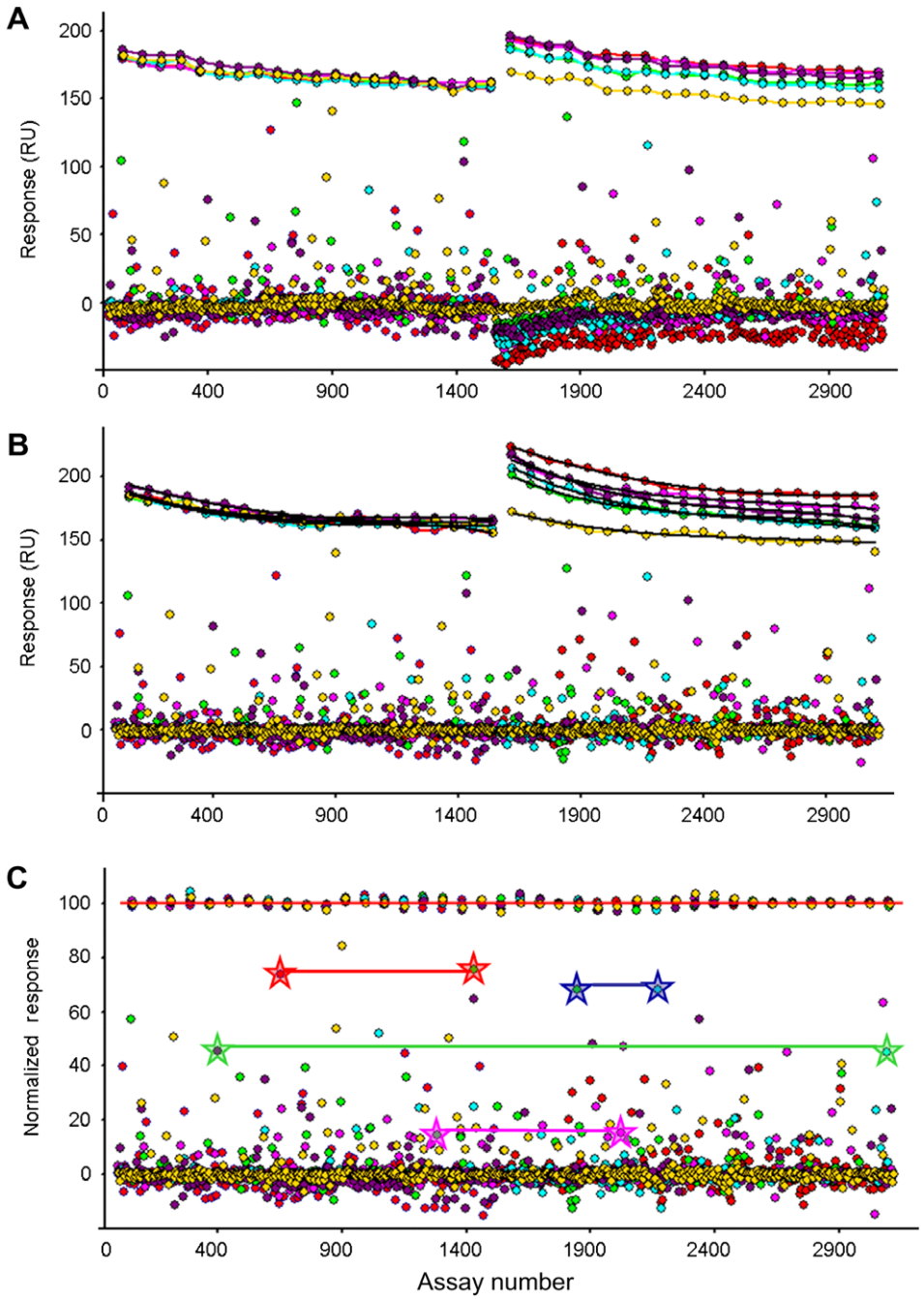

Fig. 8. Response intensities from Fig. 7 plotted against injection number. Responses in panel A are double referenced, those in panel B are baseline corrected, and those in panel C have been normalized for decay in activity of the target surface. In each panel, the data points shown in yellow, teal, green, red, pink, and purple depict the responses from the six flow cells, and the sulpiride replicates from each flow cell are indicated by the colored lines. In panels A and B, the breaks apparent midway through the screen are due to the preparation of a freshly captured target surface. The stars and connecting lines in panel C highlight the replicate responses of selected known CAII binders. (For interpretation of the references to color in this figure legend, the reader is referred to the Web version of this article.)

example, the kinetics of potential hits are rarely limited by transport issues. In fact, one would be delighted to find a compound that bound so tightly to the target that the binding responses became complex; in a way, a complex profile could be further evidence that binding was specific. But we believe that it is important to present potential limitations of all new technologies so that they may be properly evaluated.

The AP-3000 is capable of testing 10 384-well plates in 24 h when running in its fastest mode (shortest injection and washing times). It is important to realize that the total number of samples analyzed per sensor stick depends on the number of washing/regeneration steps used in an assay. This limitation relates to docking of the pipette tips into the flow cell injection ports. A fixed number of docking steps per stick is employed because of the life time of the plastic docking ports. Using the minimum number of washing steps provides the highest throughput, making it possible to analyze five 384-well plates with one sensor stick. Increasing the number of washing steps will decrease the number of samples that can be evaluated per sensor stick. The AP-3000 software assigns the number of injections per stick based on the assay protocol and automatically prepares new sensor sticks when needed.

Initially, we were coming from a mind-set of wanting to use a sensor surface until it was no longer active, so it took a little time to get accustomed to the idea of needing to create a new surface halfway through an experiment. But because the AP-3000 automatically generates a new sensor stick, this became less of an issue the more we worked with the instrument. Also, even within our CAII fragment-screening study, we could see the benefit of generating a fresh target surface. Certainly, it can be essential if less stable target proteins are being studied; in these cases, the speed of the AP-3000, combined with the ability to automatically generate new surfaces, becomes a definite advantage.

Because the AP-3000 was designed from the outset as a rapid sampling screening platform, we were worried that setting up the instrument to run a set of 10 plates (of nearly 4000 samples) would be daunting. Instead, it was surprisingly straightforward. And the available high-capacity SA surfaces, combined with the AP-3000's good signal-to-noise ratio and high throughput, make it a suitable system for drug-screening applications.

Appendix A. Supplementary data

Supplementary data associated with this article can be found, in the online version, at doi:10.1016/j.ab.2010.03.043.

References

[1] R.L. Rich, D.G. Myszka, BIACORE J: a new platform for routine biomolecular interaction analysis, J. Mol. Recogn. 14 (2001) 223–228.
[2] D.G. Myszka, Analysis of small molecule interactions using Biacore S51 technology, Anal. Biochem. 329 (2004) 316–323.
[3] P. Säfsten, S.L. Klakamp, A.W. Drake, R. Karlsson, D.G. Myszka, Screening antibody–antigen interactions in parallel using Biacore A100, Anal. Biochem. 353 (2006) 181–190.
[4] T. Bravman, V. Bronner, K. Lavie, A. Notcovich, G.A. Papalia, D.G. Myszka, Exploring "one-shot" kinetics and small molecule analysis using the ProteOn XPR36 array biosensor, Anal. Biochem. 358 (2006) 281–288.
[5] G.A. Papalia, M. Baer, K. Luehrsen, H. Nordin, P. Flynn, D.G. Myszka, High-resolution characterization of antibody fragment/antigen interactions using Biacore T100, Anal. Biochem. 359 (2006) 112–119.
[6] R.L. Rich, M.J. Cannon, J. Jenkins, P. Pandian, S. Sundaram, R. Magyar, J. Brockman, J. Lambert, D.G. Myszka, Extracting kinetic rate constants from surface plasmon resonance array systems, Anal. Biochem. 373 (2008) 112–120.
[7] M. Naya, N. Mori, T. Kimura, H. Ohtsuka, T. Kubo, H. Shimizu, Extremely high signal-to-noise ratio surface plasmon resonance sensor using a monolithic prism sensor chip, J. Nanophoton. 1 (2007) 011596.
[8] T. Nishio, K. Kuruma, T. Ezoe, N. Ogura, S. Yamashita, K. Hayashi, Development of label-free affinity perceptive system AP-3000, Fujifilm Res. Dev. 53 (2008) 29–35.
[9] D.G. Myszka, Y.N. Abdiche, F. Arisaka, O. Byron, E. Eisenstein, P. Hensley, J.A. Thomson, C.R. Lombardo, F. Schwarz, W. Stafford, M.L. Doyle, The ABRF–MIRG'02 Study: assembly state, thermodynamic, and kinetic analysis of an enzyme/inhibitor interaction, J. Biomol. Tech. 14 (2003) 247–269.
[10] I. Navratilova, G.A. Papalia, R.L. Rich, D. Bedinger, S. Brophy, B. Condon, T. Deng, A.W. Emerick, H.-W. Guan, T. Hayden, T. Heutmekers, B. Hoorelbeke, M.C. McCroskey, M.M. Murphy, T. Nakagawa, F. Parmeggiani, X. Qin, S. Rebe, N. Tomasevic, T. Tsang, M.B. Waddell, F.F. Zhang, S. Leavitt, D.G. Myszka, Thermodynamic benchmark study with Biacore technology, Anal. Biochem. 364 (2007) 67–77.
[11] M.J. Cannon, G.A. Papalia, I. Navratilova, R.J. Fisher, L.R. Roberts, K.M. Worthy, A.G. Stephen, G.R. Marchesini, E.J. Collins, D. Casper, H. Qiu, D. Satpaev, S.F. Liparoto, D.A. Rice, I.I. Gorshkova, R.J. Darling, D.B. Bennett, M. Sekar, E. Hommema, A.M. Liang, E.S. Day, J. Inman, S.M. Karlicek, S.J. Ullrich, D. Hodges, T. Chu, E. Sullivan, J. Simpson, A. Rafique, B. Luginbühl, S. Nyholm Westin, M. Bynum, P. Cachia, Y.-J. Li, D. Kao, D.G. Myszka, Comparative analyses of a small molecule/enzyme interaction by multiple users of Biacore technology, Anal. Biochem. 330 (2004) 98–113.
[12] D.G. Myszka, Improving biosensor analysis, J. Mol. Recogn. 12 (1999) 279–284.
[13] G.A. Papalia, S. Leavitt, M.A. Bynum, P.S. Katsamba, R. Wilton, H. Qiu, M. Steukers, S. Wang, L. Bindu, S. Phogat, A.M. Giannetti, T.E. Ryan, V.A. Pudlak, K. Matusiewicz, K.M. Michelson, A. Nowakowski, A. Pham-Baginski, J. Brooks, B. Tieman, B.D. Bruce, M. Vaughn, M. Baksh, Y.H. Cho, M. De Wit, A. Smets, J. Vandersmissen, L. Michiels, D.G. Myszka, Comparative analysis of 10 small molecules binding to carbonic anhydrase II by different investigators using Biacore technology, Anal. Biochem. 359 (2006) 94–105.
[14] T.A. Morton, D.G. Myszka, Kinetic analysis of macromolecular interactions using surface plasmon resonance biosensors, Methods Enzymol. 295 (1998) 268–295.
[15] R.L. Rich, D.G. Myszka, Grading the commercial optical biosensor literature – class of 2008: "The Mighty Binders", J. Mol. Recogn. 23 (2010) 1–64.